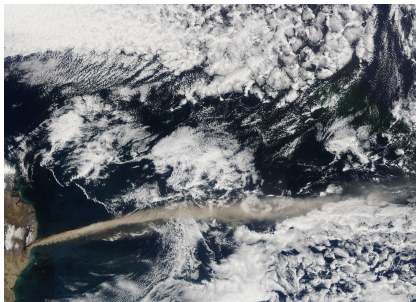


# Tracer Advection I

## Atmospheric tracer transport & design philosophies

Peter Hjort Lauritzen

Atmospheric Modeling and Predictability Section (AMP)  
Climate and Global Dynamics Division (CGD)  
NCAR Earth System Laboratory (NESL)  
National Center for Atmospheric Research (NCAR)



**DCMIP Summer School**

Picture: Eruption of Iceland's Eyjafjallajökull volcano (NASA-MODIS)

- 1 Continuity equation's in climate models
- 2 Desirable properties for transport schemes intended for climate applications
  - Mass-conservation, shape-preservation, multi-tracer efficiency, ...
  - Preservation of pre-existing functional relations (correlations) between species
- 3 A semi-Lagrangian view on finite-volume schemes

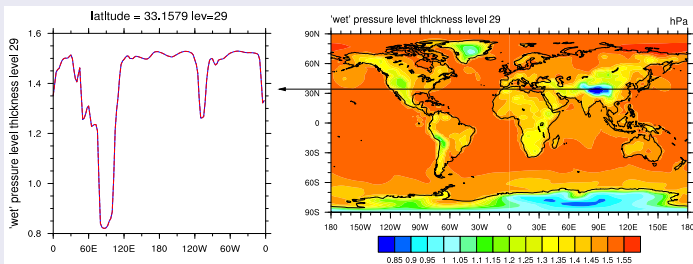
# Continuity equations in climate models: dry air

Continuity equation for dry air mass

$$\frac{\partial \rho}{\partial t} + \nabla \cdot (\rho \vec{v}) = 0,$$

where  $\vec{v}$  is the velocity field and  $\rho$  density.

- Mass of dry air  $\approx N_2$  (ca. 78.08%),  $O_2$  (ca. 20.95%),  $Ar$  (ca. 0.93%),  $CO_2$  (at present ca. 0.038%); these well-mixed gases make up 99.998% of the volume of dry air
- Trenberth and Smith (2005) estimated that the mass of dry air corresponds to a surface pressure of 983.05 hPa and it varies less than 0.01 hPa based on changes in atmospheric composition.
- $\Rightarrow$  to a very good approximation there are no source/sink terms on the right-hand side of continuity equation for dry air.



## Continuity equations for water species

$$\frac{\partial (\rho q_i)}{\partial t} + \nabla \cdot (\rho q_i \vec{v}) = P_{\rho q_i},$$

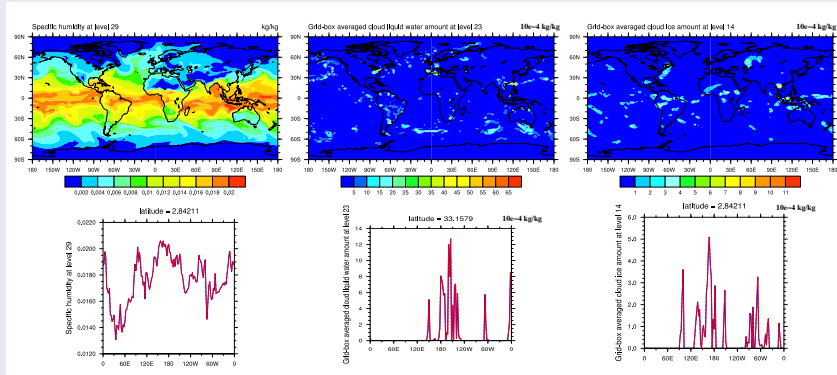
where  $q_i$  are dry mixing ratios<sup>a</sup> [ $m_i^{(d)}/m^{(d)}$ ] and  $P$  represent source and sink terms.

- $q_i$ : water vapor, cloud liquid and cloud ice.
  - 99% of the total weight of the atmosphere is the mass of dry air. The remaining 1% is approximately the mass of water (large local variations though!)
- $q_i$ : Meso-scale models also have prognostic rain, snow, graupel, ...
  - If rain, snow, graupel, etc. are diagnostic it is assumed that they fall to the ground in one physics time-step!

---

<sup>a</sup>the subtleties between using 'dry' and 'wet' mixing ratios is not discussed here - see, e.g., Lauritzen et al. (2011b)

# Continuity equations in climate models: water



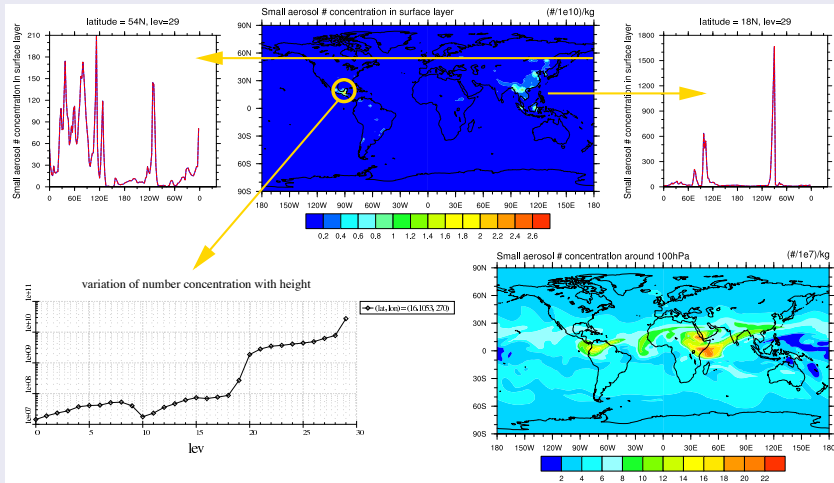
Very 'oscillatory' fields:

- Production/loss terms are large, however, clouds (e.g., 'ice clouds' such as Cirrus) can have lifetimes on the order of days
- Transport operator must not produce negative values.
- Overshooting in water vapor, for example, can trigger irreversible physical processes.

In other words: the transport scheme should be **shape-preserving** with respect to  $q$ .

# Continuity equations in climate models: aerosols

- Microphysics: continuity equations for aerosol number and mass concentrations
  - CAM5 physics: 22 aerosol continuity equations (particulate organic matter, dust, sea salt, secondary organic aerosols, ...)



# Continuity equations in climate models: chemistry

- Chemistry: continuity equations for chemical species
  - CAM-chem: approximately 127 continuity equations (ozone, chlorine compounds, bromine, ...) ... some highly reactive and some long-lived

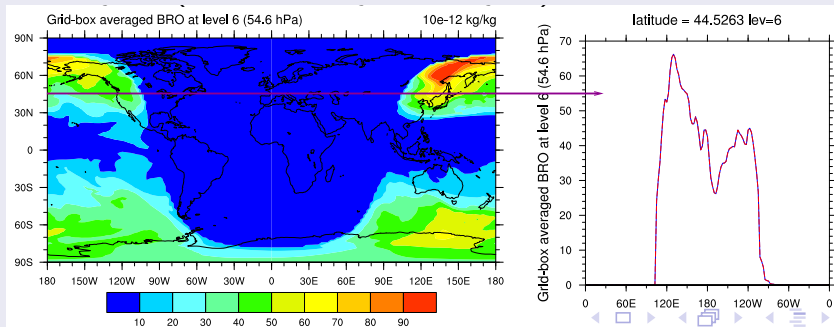


Figure: Bromine has a strong diurnal cycle (produced by photolysis)

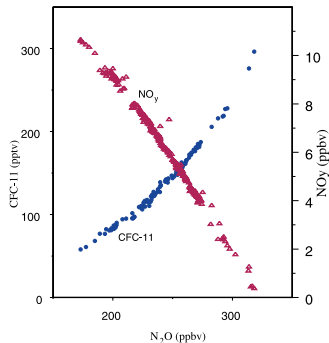
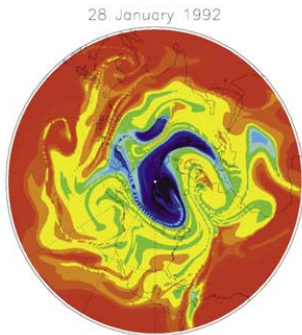
Important properties of transport schemes intended for atmospheric models:

- The number of prognostic continuity equations in climate and chemistry-climate models is increasing fast to accommodate more advanced physical parameterizations (e.g., microphysics), online chemistry, ....  
  
⇒ multi-tracer efficiency is becoming increasingly important (closely tied to compute platform)!
- Atmospheric tracer fields can have very large gradients:
  - Shape-preservation is paramount!
  - Preservation of gradients is important
- Inherent conservation of mass is desirable, in particular, to consistently enforce shape-preservation and tracer-air mass consistency.
- Optimal preservation of pre-existing functional relationships (correlations)

# Correlations between longlived species in the stratosphere

*Relationships between long-lived stratospheric tracers, manifested in similar spatial structures on scales ranging from a few to several thousand kilometers, are displayed most strikingly if the mixing ratio of one is plotted against another, when the data collapse onto remarkably compact curves. - Plumb (2007)*

*E.g., nitrous oxide ( $N_2O$ ) against 'total odd nitrogen' ( $NO_y$ ) or chlorofluorocarbon (CFC's)*

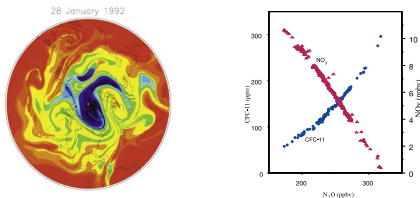


Figures from Plumb (2007).

# Correlations between longlived species in the stratosphere

*Relationships between long-lived stratospheric tracers, manifested in similar spatial structures on scales ranging from a few to several thousand kilometers, are displayed most strikingly if the mixing ratio of one is plotted against another, when the data collapse onto remarkably compact curves. - Plumb (2007)*

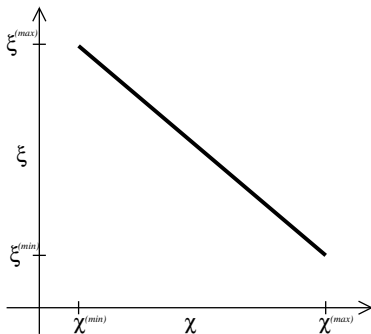
*E.g., nitrous oxide ( $N_2O$ ) against 'total odd nitrogen' ( $NO_y$ ) or chlorofluorocarbon (CFC's)*



Similarly:

- The total of chemical species within some chemical family may be preserved following an air parcel although the individual species have a complicated relation to each other and may be transformed into each other through chemical reactions (e.g., total chlorine)
- Aerosol-cloud interactions (Ovtchinnikov and Easter, 2009)

**The transport operator should ideally not perturb pre-existing functional relationships**

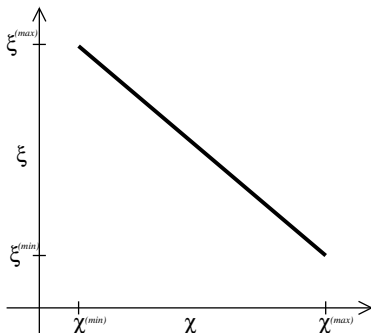


Analytical pre-existing functional relationship curve  $\psi$  (linear)

$$\xi = \psi(\chi) = a \cdot \chi + b, \quad \chi \in [\chi^{(min)}, \chi^{(max)}],$$

where  $a$  and  $b$  are constants, and  $\chi$  and  $\xi$  are the mixing ratios of the two tracers

# Analyzing scatter plots



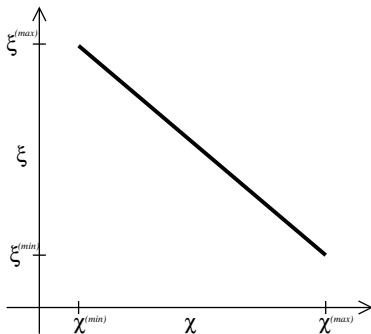
Analytical pre-existing functional relationship curve  $\psi$  (linear)

$\chi$  and  $\xi$  are transported separately by the transport scheme

$$\chi_k^{n+1} = \mathcal{T}(\chi_j^n), \quad j \in \mathcal{H},$$

$$\xi_k^{n+1} = \mathcal{T}(\xi_j^n), \quad j \in \mathcal{H},$$

where  $\mathcal{T}$  is the transport operator and  $\mathcal{H}$  the set of indices defining the 'halo' for  $\mathcal{T}$ .



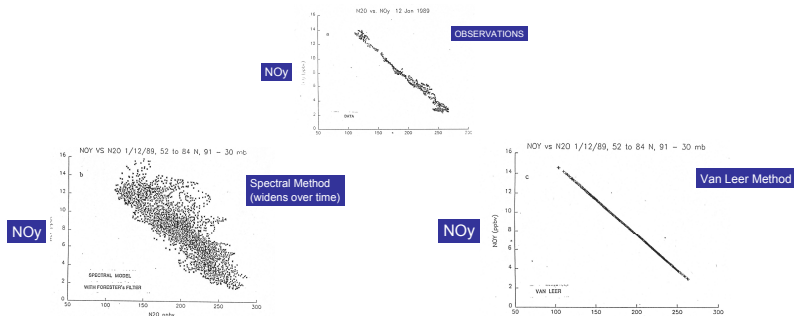
Analytical pre-existing functional relationship curve  $\psi$  (linear)

If  $\mathcal{T}$  is 'semi-linear' then linear pre-existing functional relations are preserved:

$$\xi_k^{n+1} = \mathcal{T}(\xi_j^n) = \mathcal{T}(a\chi_j^n + b) = a\mathcal{T}(\chi_j^n) + b\mathcal{T}(1) = a\mathcal{T}(\chi_j^n) + b = a\chi_k^{n+1} + b.$$

→ If transport operator is non-linear the relationship might be violated.

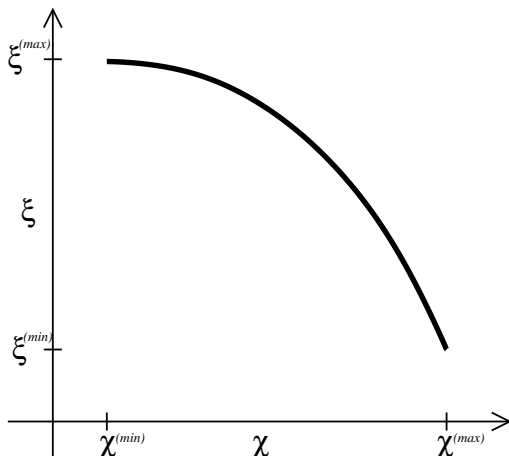
# Analyzing scatter plots



Figures from R.Rood's talk at the 2008 NCAR ASP colloquium

Analytical pre-existing functional relationship curve  $\psi$  (linear)

→ carefully designed finite-volume schemes are 'semi-linear' even with limiters/filters!  
(Thuburn and McIntyre, 1997; Lin and Rood, 1996)

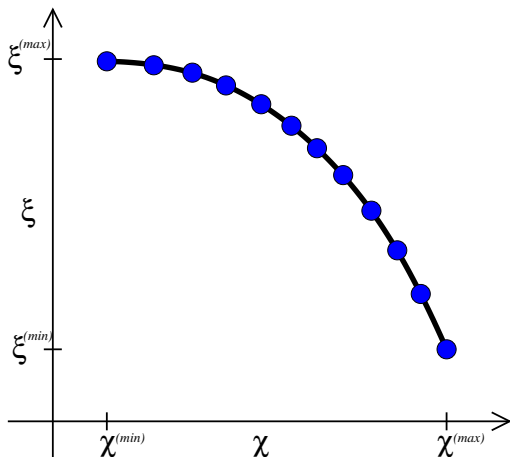


Analytical pre-existing functional relationship curve  $\psi$

$$\xi = \psi(\chi) = a \cdot \chi^2 + b,$$

where  $a$  and  $b$  are constants so that  $\psi$  is concave or convex in  $[\chi^{(min)}, \chi^{(max)}]$

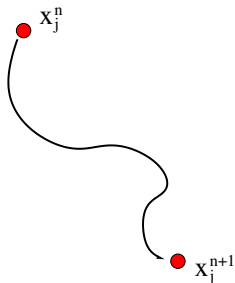
# Analyzing scatter plots



Discrete pre-existing functional relation (initial condition)

$$\xi_k = \psi(\chi_k) = a \cdot (\chi_k)^2 + b, \quad k = 1, \dots, K,$$

where  $a$  and  $b$  are constants so that  $\psi$  is concave or convex in  $[\chi^{(min)}, \chi^{(max)}]$

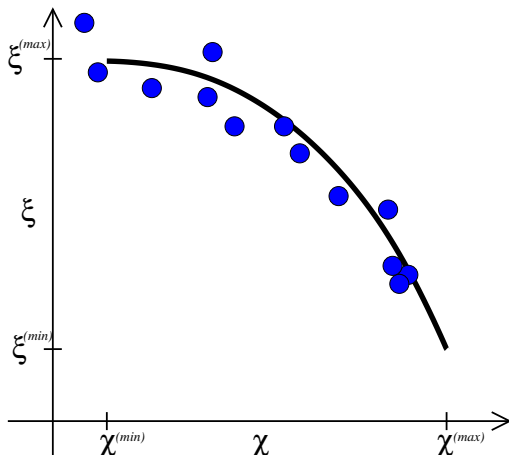


A fully Lagrangian model will maintain pre-existing functional relation

$$\chi_k^{n+1} = \chi_k^n, \quad \xi_k^{n+1} = \xi_k^n$$

following parcel trajectories (without 'contour-surgery' or other mixing mechanisms)

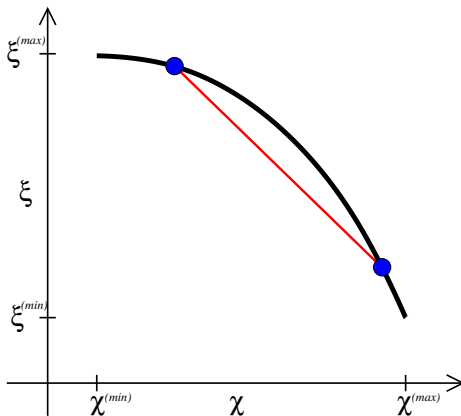
## Analyzing scatter plots



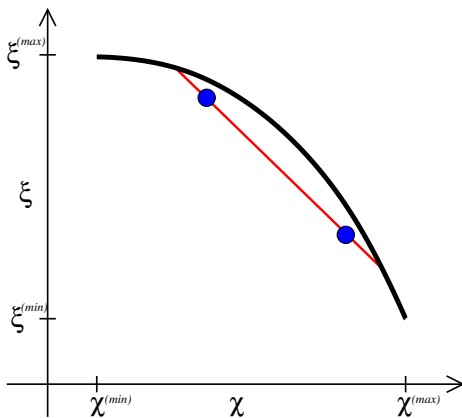
Any Eulerian/semi-Lagrangian scheme will disrupt pre-existing functional relation

$$\xi_k^{n+1} = \mathcal{T}(\xi_j^n) \neq a \cdot \mathcal{T}(\chi_j^n)^2 + b, \quad j \in \mathcal{H}$$

where  $\mathcal{T}$  is the transport operator and  $\mathcal{H}$  the set of indices defining the 'halo' for  $\mathcal{T}$ .



'Real' mixing' (when occurring) will tend to replace the functional relation by a scatter by linearly interpolating along mixing lines between pairs of points



'Real mixing' (when occurring) will tend to replace the functional relation by a scatter by linearly interpolating along mixing lines between pairs of points  
→ Ideally numerical mixing should = 'real mixing'!

However, it may be shown mathematically that schemes that exclusively introduce 'real mixing' are 1<sup>st</sup>-order schemes (Thuburn and McIntyre, 1997).

# Classification of numerical mixing on scatter plots

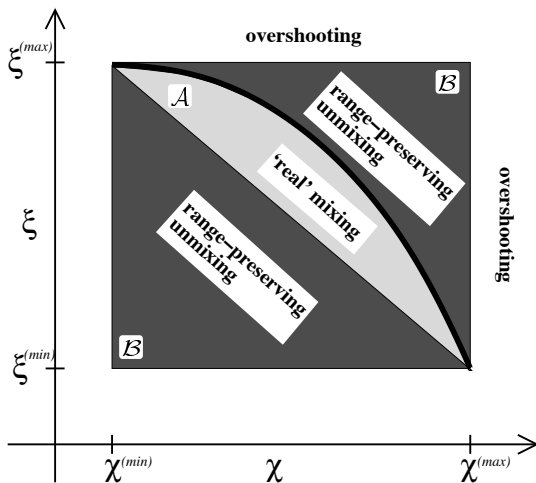
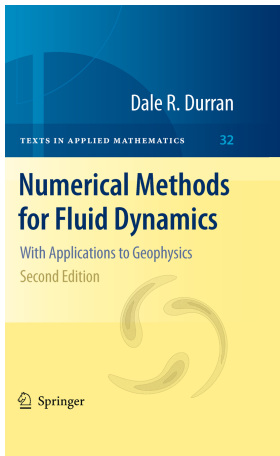


Figure from (Lauritzen and Thuburn, 2012)

Show animation from idealized test case (Lauritzen and Thuburn, 2012; Lauritzen et al., 2012)



# Derivation form

'Most fundamental equations in fluid dynamics can be derived from first principles in either a *Eulerian* form or an *Lagrangian* form' - (see, e.g., text book of Durran, 1999)

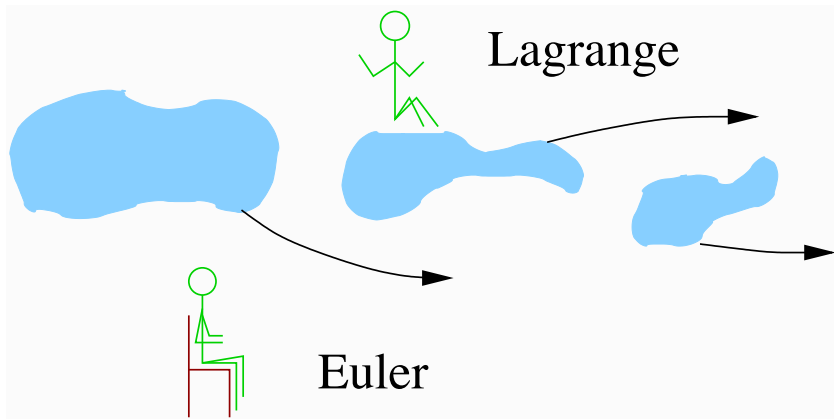
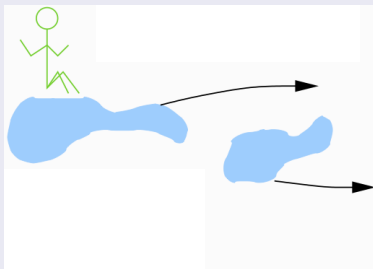


Figure courtesy of J. Thuburn.

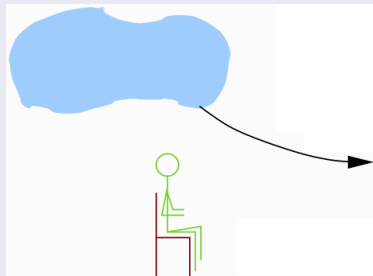
# Derivation form

Consider the continuity equation for some inert (no sources/sinks) and passive (does not feed back on the flow) tracer

## semi-Lagrangian form



## Eulerian (flux) form

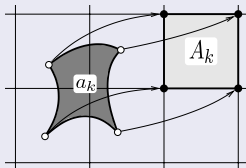


For simplicity assume a quadrilateral mesh and leave out the 'details' of spherical geometry.

- Only consider two-time-level finite-volume schemes

# Finite-volume approach: Integrate in space

## semi-Lagrangian form



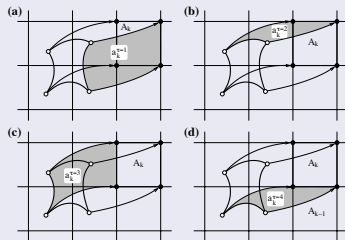
$$\frac{D}{Dt} \int_{A(t)} \psi dA = 0.$$

where  $A(t)$  is a Lagrangian<sup>†</sup> control volume and

$$\frac{D}{Dt} = \frac{\partial}{\partial t} + \vec{v} \cdot \nabla,$$

is the material/total derivative.

## Eulerian (flux-form) form



Integrate

$$\frac{\partial \psi}{\partial t} + \nabla \cdot (\psi \vec{v}) = 0$$

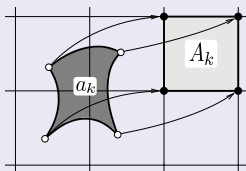
over an Eulerian control volume  $A_k$ :

$$\frac{\partial}{\partial t} \int_{A_k} \psi dA + \int_{A_k} \nabla \cdot (\psi \vec{v}) dA = 0.$$

<sup>†</sup> volume whose bounding surface moves with the local fluid velocity  $\Leftrightarrow$  volume which always contains the same material particles

# Finite-volume approach: Integrate in space

## semi-Lagrangian form



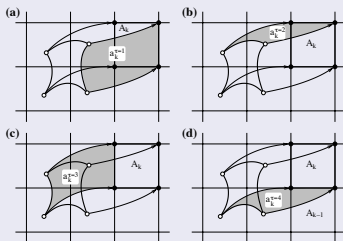
$$\frac{D}{Dt} \int_{A(t)} \psi dA = 0.$$

where  $A(t)$  is a Lagrangian<sup>†</sup> control volume and

$$\frac{D}{Dt} = \frac{\partial}{\partial t} + \vec{v} \cdot \nabla,$$

is the material/total derivative.

## Eulerian (flux-form) form



Apply divergence theorem on second term:

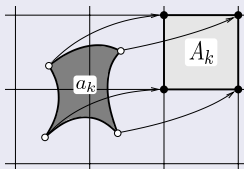
$$\frac{\partial}{\partial t} \int_{A_k} \psi dA + \oint_{\partial A_k} (\psi \vec{v}) \cdot \vec{n} dS = 0,$$

where  $\partial A_k$  is the boundary of  $A_k$  and  $\vec{n}$  the outward normal vector to  $\partial A_k$ .

→ instantaneous flux of tracer mass through boundaries of  $A_k$

<sup>†</sup> volume whose bounding surface moves with the local fluid velocity ⇔ volume which always contains the same material particles

## semi-Lagrangian form



$$\int_{A(t+\Delta t)} \psi \, dA = \int_{A(t)} \psi \, dA,$$

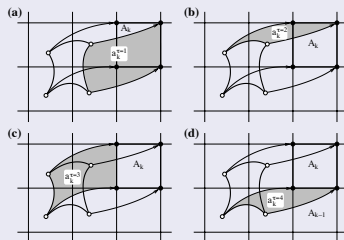
where  $\Delta t$  is time-step and  $t = n \Delta t$ .

Upstream semi-Lagrangian approach:

$$\overline{\psi}_k^{n+1} \Delta A_k = \overline{\psi}_k^n \Delta a_k,$$

where  $\overline{(\ )}$  is average value over cell.

## Eulerian (flux-form) form



Apply divergence theorem on second term:

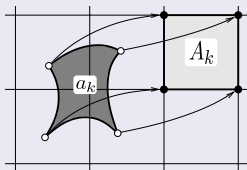
$$\frac{\partial}{\partial t} \int_{A_k} \psi \, dA + \oint_{\partial A_k} (\psi \vec{v}) \cdot \vec{n} \, dS = 0,$$

where  $\partial A_k$  is the boundary of  $A_k$  and  $\vec{n}$  the outward normal vector to  $\partial A_k$ .

→ instantaneous flux of tracer mass through boundaries of  $A_k$

# Finite-volume approach: Integrate in time

semi-Lagrangian form



$$\int_{A(t+\Delta t)} \psi dA = \int_{A(t)} \psi dA,$$

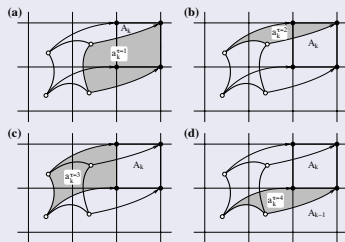
where  $\Delta t$  is time-step and  $t = n \Delta t$ .

Upstream semi-Lagrangian approach:

$$\bar{\psi}_k^{n+1} \Delta A_k = \bar{\psi}_k^n \Delta a_k,$$

where  $\bar{(\ )}$  is average value over cell.

Eulerian (flux-form) form



$$\frac{\partial}{\partial t} \int_{A_k} \psi dA + \oint_{\partial A_k} (\psi \vec{v}) \cdot \vec{n} dS = 0,$$

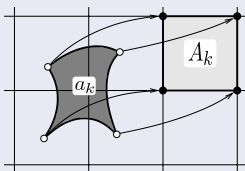
$$\bar{\psi}^{n+1} \Delta A_k = \bar{\psi}^n \Delta A_k +$$

$$\int_{n\Delta t}^{(n+1)\Delta t} \left[ \oint_{\partial A_k} (\psi \vec{v}) \cdot \vec{n} dS \right] dt = 0,$$

→ flux of tracer mass through boundaries of  $A_k$  during  $t \in [n\Delta t, (n+1)\Delta t]$

# Finite-volume approach:

## semi-Lagrangian form



$$\int_{A(t+\Delta t)} \psi dA = \int_{A(t)} \psi dA,$$

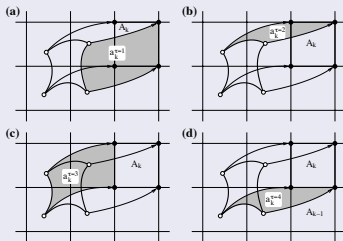
where  $\Delta t$  is time-step and  $t = n \Delta t$ .

Upstream semi-Lagrangian approach:

$$\overline{\psi}_k^{n+1} \Delta A_k = \overline{\psi}_k^n \Delta a_k,$$

where  $\overline{(\ )}$  is average value over cell.

## Eulerian (flux-form) form



$$\overline{\psi}_k^{n+1} \Delta A_k = \overline{\psi}_k^n \Delta A_k - \sum_{\tau=1}^4 F_k^{(\tau)},$$

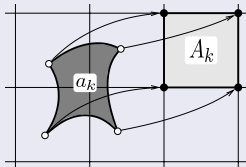
where

$$F_k^{(\tau)} = s_k^{(\tau)} \int_{a_k^{(\tau)}} \psi^n(x, y) dA.$$

is flux of mass through face  $\tau$  during  $\Delta t$ ,  
and  $s_k^{(\tau)} = \pm 1$

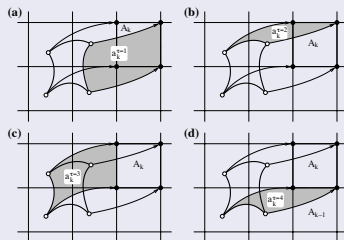
# Finite-volume approach:

## semi-Lagrangian form



$$\bar{\psi}_k^{n+1} \Delta A_k = \bar{\psi}_k^n \Delta a_k,$$

## Eulerian (flux-form) form



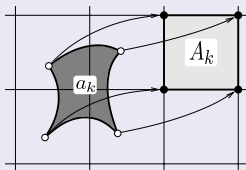
$$\bar{\psi}_k^{n+1} \Delta A_k = \bar{\psi}_k^n \Delta A_k - \sum_{\tau=1}^4 F_k^{(\tau)},$$

Note equivalence between Lagrangian cell-integrated and Eulerian flux-form continuity equations:

$$\Delta A_k - \sum_{\tau=1}^4 \left( s_k^{(\tau)} \Delta a_k^{(\tau)} \right) = \Delta a_k.$$

i.e. the areas involved in Eulerian forecast equals upstream Lagrangian area  $a_k$ .

## semi-Lagrangian form



$$\bar{\psi}_k^{n+1} \Delta A_k = \bar{\psi}_k^n \Delta a_k,$$

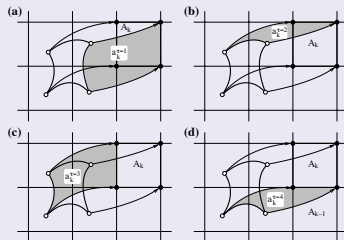
Define a global piecewise continuous reconstruction function

$$\psi(x, y) = \sum_{k=1}^N I_{A_k} \psi_k(x, y),$$

where  $I_{A_k}$  is the indicator function

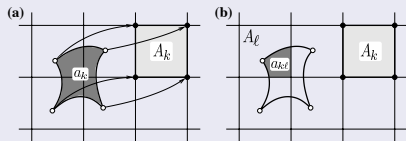
$$I_{A_k} = \begin{cases} 1, & (x, y) \in A_k, \\ 0, & (x, y) \notin A_k. \end{cases}$$

## Eulerian (flux-form) form



$$\bar{\psi}_k^{n+1} \Delta A_k = \bar{\psi}_k^n \Delta A_k - \sum_{\tau=1}^4 F_k^{(\tau)},$$

## semi-Lagrangian form



$$\bar{\psi}_k^{n+1} \Delta A_k = \bar{\psi}_k^n \Delta a_k,$$

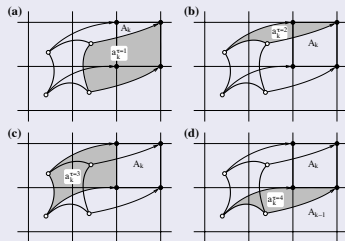
$$\bar{\psi}_k^{n+1} \Delta A_k = \sum_{\ell=1}^{L_k} \int_{a_{k\ell}} \psi_\ell^n(x, y) dA.$$

where  $a_{k\ell}$  is the non-empty overlap area

$$a_{k\ell} = a_k \cap A_\ell, \quad a_{k\ell} \neq \emptyset; \quad \ell = 1, \dots, L_k,$$

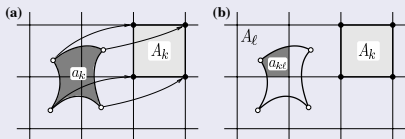
where  $N$  is the number of cells in the domain and  $L_k$  number of overlap areas.

## Eulerian (flux-form) form



$$\bar{\psi}_k^{n+1} \Delta A_k = \bar{\psi}_k^n \Delta A_k - \sum_{\tau=1}^4 F_k^{(\tau)},$$

## semi-Lagrangian form



$$\bar{\psi}_k^{n+1} \Delta A_k = \bar{\psi}_k^n \Delta a_k,$$

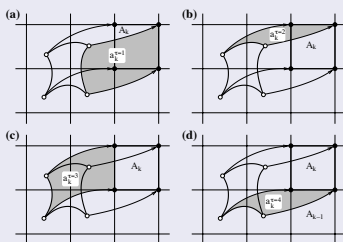
$$\bar{\psi}_k^{n+1} \Delta A_k = \sum_{\ell=1}^{L_k} \int_{a_{k\ell}} \psi_\ell^n(x, y) dA.$$

where  $a_{k\ell}$  is the non-empty overlap area

$$a_{k\ell} = a_k \cap A_\ell, \quad a_{k\ell} \neq \emptyset; \quad \ell = 1, \dots, L_k,$$

where  $N$  is the number of cells in the domain and  $L_k$  number of overlap areas.

## Eulerian (flux-form) form



$$\bar{\psi}_k^{n+1} \Delta A_k = \bar{\psi}_k^n \Delta A_k - \sum_{\tau=1}^4 F_k^{(\tau)},$$

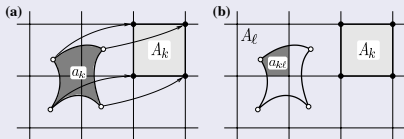
$$F_k^{(\tau)} = \sum_{\ell=1}^{L_k^{(\tau)}} \int_{a_{k\ell}} \psi_\ell^n(x, y) dA,$$

where  $L_k^{(\tau)}$  is number of non-empty 'flux' overlap areas for face  $\tau$ .

**Note that in general:**  $L_k \ll \sum_{\tau=1}^4 L_k^{(\tau)}$

# Finite-volume approach: Conditions for inherent mass-conservation

## semi-Lagrangian form



$$\bar{\psi}_k^{n+1} \Delta A_k = \bar{\psi}_k^n \Delta a_k,$$

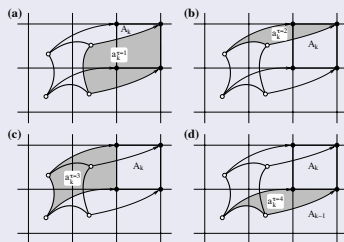
- $a_k$ 's span  $\Omega$  without gaps/overlaps

$$\bigcup_{k=1}^N a_k = \Omega, \text{ and } a_k \cap a_\ell = \emptyset \forall k \neq \ell.$$

- Sub-grid-scale representation of  $\psi$  must integrate to cell-average mass

$$\int_{A_k} \psi_k^n(x, y) dA = \bar{\psi}_k^n \Delta A_k,$$

## Eulerian (flux-form) form



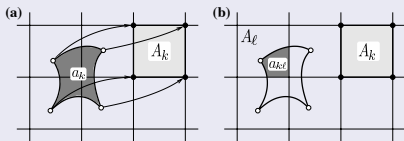
$$\bar{\psi}_k^{n+1} \Delta A_k = \bar{\psi}_k^n \Delta A_k - \sum_{\tau=1}^4 F_k^{(\tau)},$$

- Fluxes for 'shared' faces must cancel, e.g.,

$$F_k^{(3)} = -F_{k-1}^{(1)}$$

**Any flux, even highly inaccurate fluxes, will NOT violate mass-conservation!**

## semi-Lagrangian form

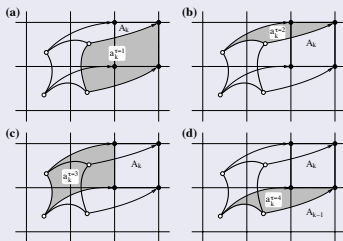


$$\bar{\psi}_k^{n+1} \Delta A_k = \bar{\psi}_k^n \Delta a_k,$$

The *only* direct way of enforcing shape-preservation is to filter the sub-grid-scale distribution  $\bar{\psi}_k^n(x, y)$ :

- fully 2D filters (Barth and Jespersen, 1989)
- 1D filters for cascade schemes (Colella and Woodward, 1984; Zerroukat et al., 2005; Lin and Rood, 1996)

## Eulerian (flux-form) form

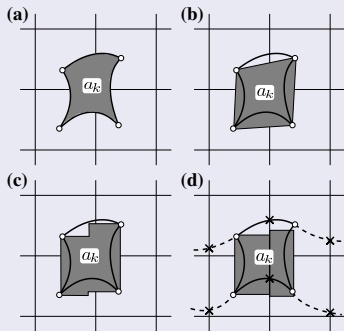


$$\bar{\psi}_k^{n+1} \Delta A_k = \bar{\psi}_k^n \Delta A_k - \sum_{\tau=1}^4 F_k^{(\tau)},$$

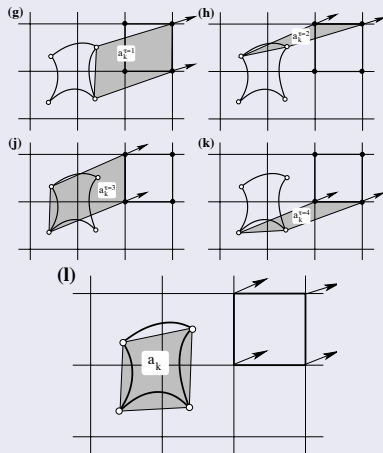
Shape-preservation can be enforced by

- blending monotone and high-order fluxes (e.g., Flux-Corrected Transport Zalesak, 1979)
- making  $\bar{\psi}_k^n(x, y)$  shape-preserving (Barth and Jespersen, 1989)

# Finite-volume approach: Area approximation

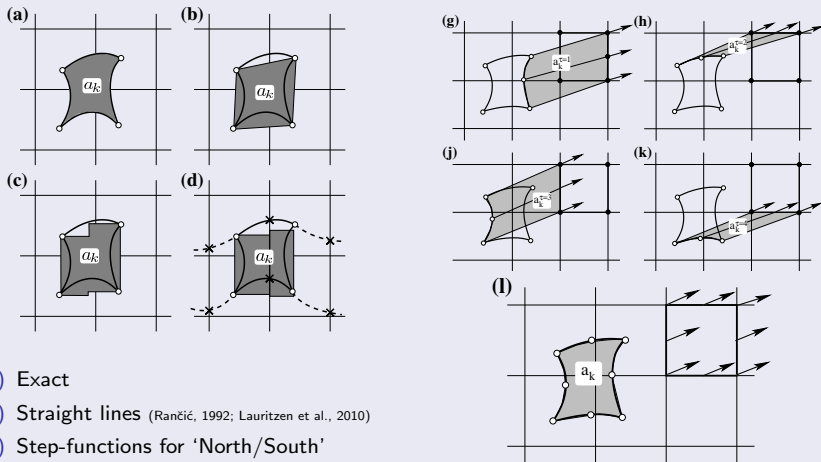


- (a) Exact
- (b) Straight lines (Rančić, 1992; Lauritzen et al., 2010)
- (c) Step-functions for 'North/South' faces & straight lines parallel to 'longitudes' for 'East/West' faces (Nair and Machenhauer, 2002).
- (d) Cascade (flow-split) (Nair et al., 2002; Zerroukat et al., 2002)



- (g-k) Quadrilateral flux-areas (Dukowicz and Baumgardner, 2000; Harris et al., 2010)
- (l) 'Effective' departure area

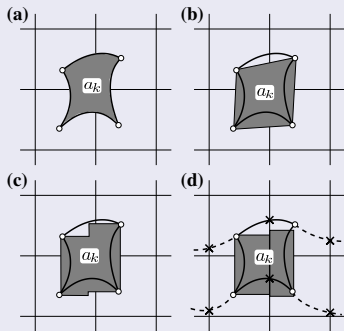
# Finite-volume approach: Area approximation



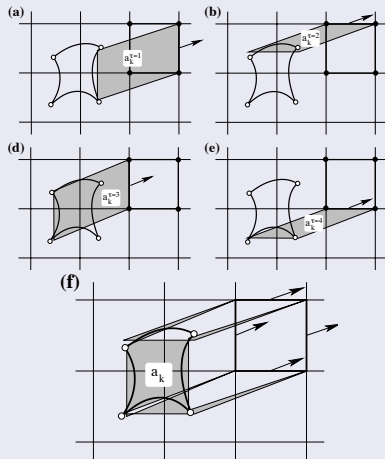
- (a) Exact
- (b) Straight lines (Rančić, 1992; Lauritzen et al., 2010)
- (c) Step-functions for 'North/South' faces & straight lines parallel to 'longitudes' for 'East/West' faces (Nair and Machenhauer, 2002).
- (d) Cascade (flow-split) (Nair et al., 2002; Zerroukat et al., 2002)

- (g-k) 'Curved' (parabolic) flux-areas (Ullrich et al., 2012)
- (l) 'Effective' departure area

# Finite-volume approach: Area approximation



- (a) Exact
- (b) Straight lines (Rančić, 1992; Lauritzen et al., 2010)
- (c) Step-functions for 'North/South' faces & straight lines parallel to 'longitudes' for 'East/West' faces (Nair and Machenhauer, 2002).
- (d) Cascade (flow-split) (Nair et al., 2002; Zerroukat et al., 2002)



- (g-k) Parallelogram flux-areas (Miura, 2007; Skamarock and Menchaca, 2010)
- (l) 'Effective' departure area

# Finite-volume approach: Area approximation

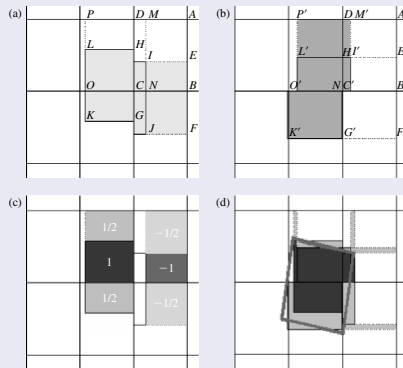
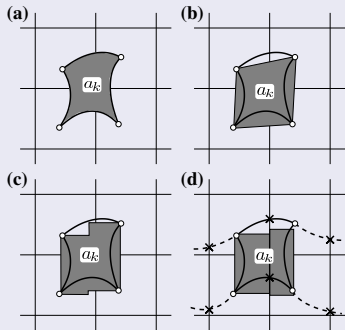
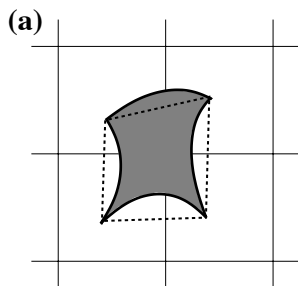


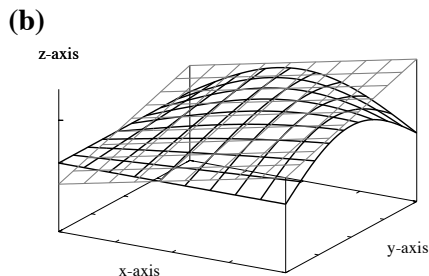
Figure from Machenhauer et al. (2009)

- (a) Exact
- (b) Straight lines (Rančić, 1992; Lauritzen et al., 2010)
- (c) Step-functions for 'North/South' faces & straight lines parallel to 'longitudes' for 'East/West' faces (Nair and Machenhauer, 2002).
- (d) Cascade (flow-split) (Nair et al., 2002; Zerroukat et al., 2002)

- (a-c) Dimensionally split scheme (Lin and Rood, 1996):  
Flux-areas area combinations of rectangles aligned with grid lines
- (d) 'Effective' departure area



*Geometric error*



*Reconstruction error*

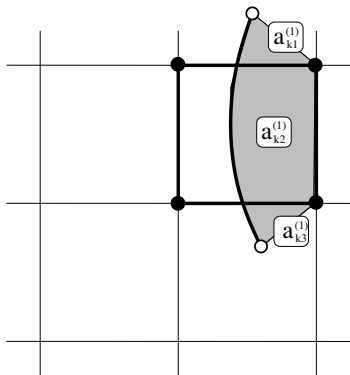
- **'geometric error'**: how well is the upstream Lagrangian area / flux areas approximated
- **'reconstruction error'**: how well is the sub-grid-scale distribution approximated

(methods for reconstructions was discussed in P.A. Ullrich's lecture 1)

Typically:

- for lower-order reconstruction functions the 'reconstruction error'  $\gg$  'geometric error'
- the smaller the Courant number ( $\Delta t$ ) the smaller the 'geometric error'
- for higher-order reconstruction functions and shear flows (deformational) the 'geometric error' can be significant (Ullrich et al., 2012)

Recall: we can do anything we want with the fluxes as long as  $F_k^{(3)} = -F_{k-1}^{(1)}$



'Rigorous' flux for face 1 ( $\tau = 1$ ):

$$F_k^{(1)} = \sum_{\ell=1}^3 \int_{a_{k\ell}} \psi_{\ell}^n(x, y) dA.$$

For  $\Delta t$  sufficiently small:

$$\Delta a_{k2} \gg \Delta a_{k1} \text{ and } \Delta a_{k2} \gg \Delta a_{k3}$$

→ simplify flux-integration by only using one upstream reconstruction function:

$$F_k^{(1)} \approx \mathcal{F}_k^{(1)} = \int_{a_{k1} \cup a_{k2} \cup a_{k3}} \psi_2^n(x, y) dA.$$

$\psi_2^n$  is extrapolated over  $a_{k1}$  and  $a_{k3}$ .

- note: the search for overlap areas has almost been eliminated in  $\mathcal{F}_k^{(1)}$
- $\mathcal{F}_k^{(1)}$  stable for Courant numbers approximately less than  $\frac{1}{2}$  ( $\Delta a_{k2} > \Delta a_{k1} + \Delta a_{k3}$ ) (Lauritzen et al., 2011a)
- $\mathcal{F}_k^{(1)}$  can be slightly more accurate than  $F_k^{(1)}$  (Lauritzen et al., 2011a)

The  $\eta$ -coordinate atmospheric primitive equations, neglecting dissipation and forcing terms:

$$\frac{\partial \vec{v}}{\partial t} + (\zeta + f) \hat{k} \times \vec{v} + \nabla \left( \frac{1}{2} \vec{v}^2 + \Phi \right) + \dot{\eta} \frac{\partial \vec{v}}{\partial \eta} + \frac{RT_v}{p} \nabla p = 0 \quad (1)$$

$$\frac{\partial T}{\partial t} + \vec{v} \cdot \nabla T + \dot{\eta} \frac{\partial T}{\partial \eta} - \frac{RT_v}{c_p^* p} \omega = 0 \quad (2)$$

$$\frac{\partial}{\partial t} \left( \frac{\partial p}{\partial \eta} \right) + \nabla \cdot \left( \frac{\partial p}{\partial \eta} \vec{v} \right) + \frac{\partial}{\partial \eta} \left( \dot{\eta} \frac{\partial p}{\partial \eta} \right) = 0 \quad (3)$$

$$\frac{\partial}{\partial t} \left( \frac{\partial p}{\partial \eta} q \right) + \nabla \cdot \left( \frac{\partial p}{\partial \eta} q \vec{v} \right) + \frac{\partial}{\partial \eta} \left( \dot{\eta} \frac{\partial p}{\partial \eta} q \right) = 0. \quad (4)$$

- Continuity equation for air is coupled with momentum and thermodynamic equations:
  - thermodynamic variables and other prognostic variables feed back on the velocity field
  - which, in turn, feeds back on the solution to the continuity equation.
  - Hence the continuity equation for air can not be solved in isolation and one must obey the maximum allowable time-step restrictions imposed by the fastest waves in the system.
- The passive tracer transport equation can be solved in isolation given prescribed winds and air densities, and is therefore not susceptible to the time-step restrictions imposed by the fastest waves in the system.

Continuity equation for air density  $\rho$

$$\frac{\partial \rho}{\partial t} + \nabla \cdot (\rho \vec{v}) = 0, \quad (1)$$

and a tracer with mixing ratio  $q$

$$\frac{\partial(\rho q)}{\partial t} + \nabla \cdot (\rho q \vec{v}) = 0, \quad (2)$$

- In continuous space:

$q = 1 \Rightarrow$  continuity equation for  $(\rho q)$  reduces to continuity equation for air  $(\rho)$

- It is considered desirable that discretization schemes obey this relation:

**'free-stream' preserving** or 'consistent' tracer transport.

- Note: 'complete consistency' is obtained if air density and tracer mass continuity equations are solved using the same numerical method, on the same discretization grid, and using the same **time-steps** (everything is 'in sync'!).

# Time-stepping and coupling:

semi-Lagrangian form

Eulerian (flux-form) form

Traditionally: semi-Lagrangian advection of  $\rho$  is combined with semi-implicit time-stepping:

$$\bar{\rho}_k^{n+1} = (\bar{\rho}_k^{n+1})_{exp} - \frac{\Delta t}{2} \rho_{00} (\nabla \cdot \vec{v}_k^{n+1} - \nabla \cdot \tilde{v}_k^{n+1}),$$

where

- $\rho_{00}$  a constant reference density
- $(\cdot)_{exp}$  is the explicit prediction
- $\tilde{v}^{n+1}$  velocity extrapolated to time-level  $(n+1)$

What about tracers?

- Solving continuity equation for  $(\rho q)$  explicitly

$$\bar{\rho} \bar{q}_k^{n+1} \Delta A_k = \bar{\rho} \bar{q}_k^n \Delta a_k$$

is NOT 'free-stream' preserving!

- Using 'traditional' semi-implicit approach for tracers

$$\bar{\rho} \bar{q}_k^{n+1} \Delta A_k = \bar{\rho} \bar{q}_k^n \Delta a_k - \frac{\Delta t}{2} (\rho q)_{00} (\nabla \cdot \vec{v}_k^{n+1} - \nabla \cdot \tilde{v}_k^{n+1}).$$

is problematic (Lauritzen et al., 2008).

Traditionally: semi-Lagrangian advection of  $\rho$  is combined with semi-implicit time-stepping:

$$\bar{\rho}_k^{n+1} = (\bar{\rho}_k^{n+1})_{exp} - \frac{\Delta t}{2} \left\{ \nabla \cdot \left[ (\bar{\rho}_k^{n+1})_{exp} \tilde{\mathbf{v}}_k^{n+1} \right] - \nabla \cdot \left[ (\bar{\rho}_k^n)_{exp} \tilde{\mathbf{v}}_k^{n+1} \right] \right\}.$$

where

- $\rho_{00}$  a constant reference density
- $(\cdot)_{exp}$  is the explicit prediction
- $\tilde{\mathbf{v}}^{n+1}$  velocity extrapolated to time-level  $(n + 1)$

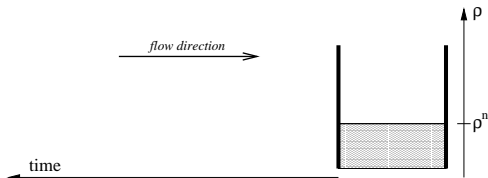
What about tracers?

- A solution is to formulate the semi-implicit terms in flux-form

$$\bar{\rho} \bar{q}_k^{n+1} = (\bar{\rho} \bar{q}_k^{n+1})_{exp} - \frac{\Delta t}{2} \left\{ \nabla \cdot \left[ (\bar{\rho} \bar{q}_k^{n+1})_{exp} \tilde{\mathbf{v}}_k^{n+1} \right] - \nabla \cdot \left[ (\bar{\rho} \bar{q}_k^n)_{exp} \tilde{\mathbf{v}}_k^{n+1} \right] \right\}.$$

so that reference states are eliminated (Wong et al., 2012)

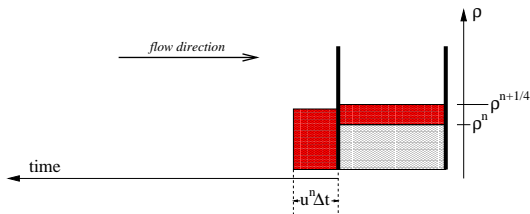
# Time-stepping and coupling: Eulerian flux-form



For efficiency, sub-cycle dynamics with respect to tracers:

- Solve continuity equation for air  $\rho$  together with momentum and thermodynamics equations.
- Repeat  $k_{split}$  times
- Brown area = average flow of mass through cell face.
- Compute time-averaged value of  $q$  across brown area using flux-form scheme:  $\overline{\overline{q}}$ .
- Flux of tracer mass:  $\overline{\overline{q}} \times \sum_{i=1}^{k_{split}} \rho^{n+i} / k_{split}$
- Yields 'free stream' preserving solution!

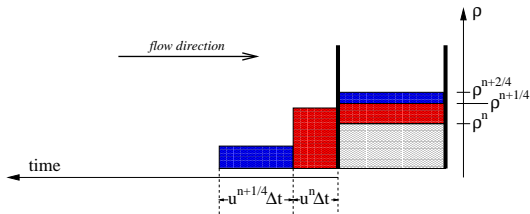
# Time-stepping and coupling: Eulerian flux-form



For efficiency, sub-cycle dynamics with respect to tracers:

- Solve continuity equation for air  $\rho$  together with momentum and thermodynamics equations.
- Repeat *ksplit* times
- Brown area = average flow of mass through cell face.
- Compute time-averaged value of  $q$  across brown area using flux-form scheme:  $\overline{\overline{q}}$ .
- Flux of tracer mass:  $\overline{\overline{q}} \times \sum_{i=1}^{ksplit} \rho^{n+i} / ksplit$
- Yields 'free stream' preserving solution!

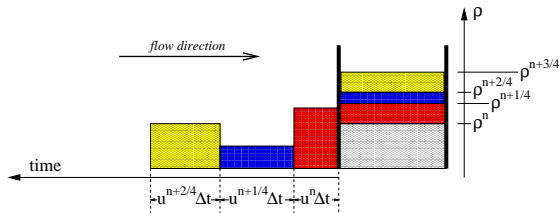
# Time-stepping and coupling: Eulerian flux-form



For efficiency, sub-cycle dynamics with respect to tracers:

- Solve continuity equation for air  $\rho$  together with momentum and thermodynamics equations.
- Repeat *ksplit* times
- Brown area = average flow of mass through cell face.
- Compute time-averaged value of  $q$  across brown area using flux-form scheme:  $\overline{\overline{q}}$ .
- Flux of tracer mass:  $\overline{\overline{q}} \times \sum_{i=1}^{ksplit} \rho^{n+i} / ksplit$
- Yields 'free stream' preserving solution!

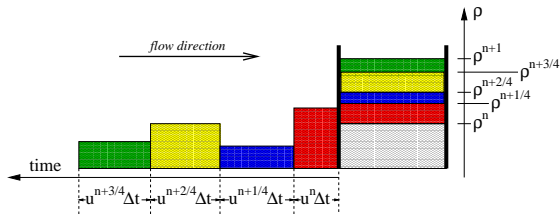
# Time-stepping and coupling: Eulerian flux-form



For efficiency, sub-cycle dynamics with respect to tracers:

- Solve continuity equation for air  $\rho$  together with momentum and thermodynamics equations.
- Repeat *ksplit* times
- Brown area = average flow of mass through cell face.
- Compute time-averaged value of  $q$  across brown area using flux-form scheme:  $\overline{\overline{q}}$ .
- Flux of tracer mass:  $\overline{\overline{q}} \times \sum_{i=1}^{ksplit} \rho^{n+i} / ksplit$
- Yields 'free stream' preserving solution!

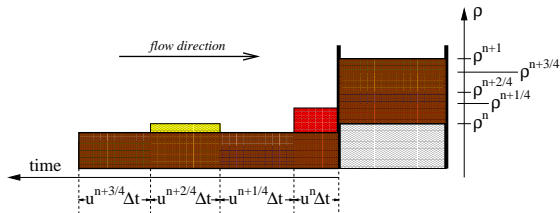
# Time-stepping and coupling: Eulerian flux-form



For efficiency, sub-cycle dynamics with respect to tracers:

- Solve continuity equation for air  $\rho$  together with momentum and thermodynamics equations.
- Repeat *ksplit* times
- Brown area = average flow of mass through cell face.
- Compute time-averaged value of  $q$  across brown area using flux-form scheme:  $\overline{\overline{q}}$ .
- Flux of tracer mass:  $\overline{\overline{q}} \times \sum_{i=1}^{ksplit} \rho^{n+i} / ksplit$
- Yields 'free stream' preserving solution!

# Time-stepping and coupling: Eulerian flux-form



For efficiency, sub-cycle dynamics with respect to tracers:

- Solve continuity equation for air  $\rho$  together with momentum and thermodynamics equations.
- Repeat *ksplit* times
- Brown area = average flow of mass through cell face.
- Compute time-averaged value of  $q$  across brown area using flux-form scheme:  $\overline{\overline{q}}$ .
- Flux of tracer mass:  $\overline{\overline{q}} \times \sum_{i=1}^{ksplit} \rho^{n+i} / ksplit$
- Yields 'free stream' preserving solution!

# Questions?



- Barth, T. and Jespersen, D. (1989). The design and application of upwind schemes on unstructured meshes. *Proc. AIAA 27th Aerospace Sciences Meeting, Reno*.
- Colella, P. and Woodward, P. R. (1984). The piecewise parabolic method (PPM) for gas-dynamical simulations. *J. Comput. Phys.*, 54:174–201.
- Dukowicz, J. K. and Baumgardner, J. R. (2000). Incremental remapping as a transport/advection algorithm. *J. Comput. Phys.*, 160:318–335.
- Durrant, D. D. (1999). *Numerical Methods for Wave Equations in Geophysical Fluid Dynamics*. Springer-Verlag.
- Harris, L. M., Lauritzen, P. H., and Mittal, R. (2010). A flux-form version of the conservative semi-Lagrangian multi-tracer transport scheme (CSLAM) on the cubed sphere grid. *J. Comput. Phys.*, 230(4):1215–1237.
- Lauritzen, P. and Thuburn, J. (2012). Evaluating advection/transport schemes using interrelated tracers, scatter plots and numerical mixing diagnostics. *Quart. J. Roy. Met. Soc.*, 138(665):906–918.
- Lauritzen, P. H., Erath, C., and Mittal, R. (2011a). On simplifying ‘incremental remap’-type transport schemes. *J. Comput. Phys.*, 230:7957–7963.
- Lauritzen, P. H., Kaas, E., Machenhauer, B., and Lindberg, K. (2008). A mass-conservative version of the semi-implicit semi-Lagrangian HIRLAM. *Q.J.R. Meteorol. Soc.*, 134.
- Lauritzen, P. H., Nair, R. D., and Ullrich, P. A. (2010). A conservative semi-Lagrangian multi-tracer transport scheme (CSLAM) on the cubed-sphere grid. *J. Comput. Phys.*, 229:1401–1424.
- Lauritzen, P. H., Skamarock, W. C., Prather, M. J., and Taylor, M. A. (2012). A standard test case suite for 2d linear transport on the sphere. *Geo. Geosci. Model Dev.*, 5:887–901.
- Lauritzen, P. H., Ullrich, P. A., and Nair, R. D. (2011b). Atmospheric transport schemes: desirable properties and a semi-Lagrangian view on finite-volume discretizations, in: P.H. Lauritzen, R.D. Nair, C. Jablonowski, M. Taylor (Eds.), Numerical techniques for global atmospheric models. *Lecture Notes in Computational Science and Engineering, Springer, 2011*, 80.
- Lin, S. J. and Rood, R. B. (1996). Multidimensional flux-form semi-Lagrangian transport schemes. *Mon. Wea. Rev.*, 124:2046–2070.
- Machenhauer, B., Kaas, E., and Lauritzen, P. H. (2009). Finite volume methods in meteorology, in: R. Temam, J. Tribbia, P. Ciarlet (Eds.), Computational methods for the atmosphere and the oceans. *Handbook of Numerical Analysis*, 14. Elsevier, 2009, pp.3-120.
- Margolin, L. G. and Shashkov, M. (2003). Second-order sign-preserving conservative interpolation (remapping) on general grids. *J. Comput. Phys.*, 184:266–298.
- Miura, H. (2007). An upwind-biased conservative advection scheme for spherical hexagonal-pentagonal grids. *Mon. Wea. Rev.*, 135:4038–4044.
- Nair, R. D. and Machenhauer, B. (2002). The mass-conservative cell-integrated semi-Lagrangian advection scheme on the sphere. *Mon. Wea. Rev.*, 130(3):649–667.
- Nair, R. D., Scroggs, J. S., and Semazzi, F. H. M. (2002). Efficient conservative global transport schemes for climate and atmospheric chemistry models. *Mon. Wea. Rev.*, 130(8):2059–2073.

- Ovtchinnikov, M. and Easter, R. C. (2009). Nonlinear advection algorithms applied to interrelated tracers: Errors and implications for modeling aerosol-cloud interactions. *Mon. Wea. Rev.*, 137:632–644.
- Plumb, R. A. (2007). Tracer interrelationships in the stratosphere. *Rev. Geophys.*, 45(RG4005).
- Rančić, M. (1992). Semi-Lagrangian piecewise bi-parabolic scheme for two-dimensional horizontal advection of a passive scalar. *Mon. Wea. Rev.*, 120:1394–1405.
- Skamarock, W. C. and Menchaca, M. (2010). Conservative transport schemes for spherical geodesic grids: High-order reconstructions for forward-in-time schemes. *Mon. Wea. Rev.*, 138:4497–4508.
- Thuburn, J. and McIntyre, M. (1997). Numerical advection schemes, cross-isentropic random walks, and correlations between chemical species. *J. Geophys. Res.*, 102(D6):6775–6797.
- Trenberth, K. E. and Smith, L. (2005). The mass of the atmosphere: A constraint on global analyses. *J. Climate*, 18:864–875.
- Ullrich, P., Lauritzen, P., and Jablonowski, C. (2012). Some considerations for high-order 'incremental remap'-based transport schemes: edges, reconstructions and area integration. *Int. J. Numer. Meth. Fluids*. revising.
- Waugh, D. W., Plumb, R. A., Elkins, J. W., Fahey, D. W., Boering, K. A., Dutton, G. S., Volk, C. M., Keim, E., Gao, R.-S., Daube, B. C., Wofsy, S. C., Loewenstein, M., Podolske, J. R., Chan, K. R., Proffitt, M. H., Kelly, K. K., Newman, P. A., and Lait, L. R. (1997). Mixing of polar vortex air into middle latitudes as revealed by tracer-tracer scatterplots. *J. Geophys. Res.*, 102(D11):119–134.
- Wong, M., Skamarock, W. C., and Lauritzen, P. H. (2012). A cell-integrated semi-implicit semi-Lagrangian shallow-water model (CSLAM-SW) with consistent treatment of inherently-conservative mass and scalar mass transport. *Mon. Wea. Rev.* in prep.
- Zalesak, S. T. (1979). Fully multidimensional flux-corrected transport algorithms for fluids. *J. Comput. Phys.*, 31:335–362.
- Zerroukat, M., Wood, N., and Staniforth, A. (2002). SLICE: A semi-Lagrangian inherently conserving and efficient scheme for transport problems. *Q. J. R. Meteorol. Soc.*, 128:2801–2820.
- Zerroukat, M., Wood, N., and Staniforth, A. (2005). A monotonic and positive-definite filter for a semi-Lagrangian inherently conserving and efficient (SLICE) scheme. *Q. J. R. Meteorol. Soc.*, 131(611):2923–2936.